Progress In Electromagnetics Research C, Vol. 124, 97–109, 2022

Sub-6 GHz Adjustable Broadband Radiation Pattern Microstrip Antenna for Wireless Communication System

Faouzi Rahmani[1, *], Naima A. Touhami[1], Abdelmounaim B. Kchairi[2], Mohammed Lamsalli[1], Nihade Taher[3], and Mohammed A. Ennasar[1]

Abstract—The present work demonstrates the design of a wideband 2×1 reconfigurable beam steering array for wireless communication systems. The designed antenna is powered by a microstrip line and consists of a two rectangular-shaped radiating elements and a rectangular planar ground. Its dimensions are as follows: $0.67\lambda 0 \times 0.53\lambda 0 \times 0.03\lambda 0$. It executes three reconfigurable operating states by turning on and off two PIN diodes to change the direction of the main beam, as well as a beam tilt ranging from ($\pm 30°$) to ($\pm 38°$). A progressive analysis in order to enhance the antenna characteristic performances is furnished. The proposed reconfigurable antenna bandwidth is 18.18% (simulated), 18.84% (theoretical), and 19.42% (measured). The presented antenna has a maximum gain of 8.62 dB (simulated) and 8.45 dB (measured), and a higher efficiency ratio of 80% to 86% over the operating band (5 GHz–6 GHz). The designed antenna is fabricated using a low loss Rogers RT5880 substrate of 2.2 relative permittivity. The simulated, theoretical, and measured results are presented and exhibit a good accord, including the S_{11} parameter and radiation patterns. In addition to the pattern reconfiguration, the obtained results are useful in order to improve the overall gain, antenna bandwidth and efficiency.

1. INTRODUCTION

In recent years, wireless technologies have been developed considerably in different areas due to the good wireless devices performance. In the antenna systems field, the design of smart antennas has attracted much interest [1, 2]. Its multi-functionality in polarization selectivity, frequency selection, and reconfiguration of the pattern makes it very adapted for different wireless systems, such as wireless sensors networks, WiMAX and WLAN wireless communication systems [3]. The adjustable pattern antenna can generate various radiation patterns at the same operating frequency. By controlling the bias voltage applied to the electronic switches, this type of antenna can ensure electrical adjustment mechanisms with electromagnetic waves multi-functional control [4]. In electronic switching elements, varactor diodes, RF-MEMSs, or PIN diodes are commonly used as typical electronic switches in reconfigurable metal surfaces [5]. Varactor diodes own nonlinear characteristics and also require complex biasing circuitry, whereas RF-MEMSs possess mechanical movement, poor reliability, and a limited life cycle which add complexity. Based on their reliability, simplicity, low cost, very low control voltage, no moving parts, high tuning speed, and linear characteristics at higher frequencies, PIN diodes are mostly chosen [6, 7].

There exist a few key techniques and approaches in the literature to take into account the pattern reconfigurability with enhanced radiation efficiency, bandwidth, and antenna gain. By monitoring four feeding ports, the antenna in [8], based on a circular patch upon which a vertical slot was etched,

Received 7 July 2022, Accepted 7 September 2022, Scheduled 17 September 2022

* Corresponding author: Faouzi Rahmani (rahmani.faouzi-etu@uae.ac.ma).

[1] Faculty of Sciences, Abdelmalek Essaadi University, Tetouan, Morocco. [2] Faculty of Science and Technology of Mohammadia, Hassan II University of Casablanca, Morocco. [3] National School of Applied Sciences, Abdelmalek Essaadi University, Tetouan, Morocco.

radiated in four different directions. The antenna in [9] was powered differentially through four feeding ports and composed of radiators and parasitic elements. Based on the control of the ON and OFF of the PIN diodes, the antenna achieved six states. Based on the switching ON either of the PIN diodes, the antenna radiation pattern in [10] would be reconfigured by orienting the main lobe in three different directions. As a result of changing the operating states of two RF MEMS switches, the antenna in [11] can radiate in three directions. Hence, in [12], by switching feeding probes for an antenna array with four elements *via* monitoring the states of varactor diodes and PIN diodes, the radiation beam can be electronically switched among five operating modes. When the varactor diodes are loaded with five different voltages, the beam of antenna in [13] can achieve five different directions. By monitoring the ON and OFF of PIN diodes, the antenna main beam in [14] can radiate in six different directions. The reconfiguration of the array diagram using the pixel method was studied in [15], and by deactivating some selected array elements, the main beam can be steered in specific directions.

In this paper, we propose a microstrip antenna array forming of two radiating elements to enhance the gain and bandwidth of the antenna, in addition to the reconfiguration of pattern. By switching the ON or OFF of two MPP4203 PIN diodes [16], the radiation beam can be dynamically switched among three operating states. Accordingly, a wide angle beams switching property ranging from ($\pm 30^\circ$) to ($\pm 38^\circ$) in an elevation plane can be performed using an inexpensive and simple technique without the need to implement supplementary conventional circuitry. The designed antenna presents good radiation characteristics along with a high gain (up to 8.62 dB) and wide bandwidth to cover the complete 5 GHz band spectrum (i.e., 5–6 GHz).

This work is structured as follows. The design evolution and working principle of the proposed antenna, the study of the effects of key geometrical parameters to achieve better performance, and the equivalent circuit model are given in Section 2. To experimentally validate the presented design, a fully functional prototype antenna is fabricated and measured, and the theoretical, measured, and simulated results are given and discussed in Section 3. The conclusion of this study is presented in Section 4.

2. DESIGN PRINCIPLES

2.1. Antenna Impedance Matching

Figure 1 illustrates the evolution of the proposed antenna design, with the related simulated S_{11} parameter results as plotted in Fig. 2(a), and simulated gain of each step is plotted in Fig. 2(b). All the studied structures are etched on a Rogers RT5880 substrate of $h = 1.57$ mm thickness, with a loss tangent of 0.0009 and relative permittivity of 2.2. The choice of the antenna geometry is very important in order to radiate in specific directions. The proposed antenna is generally constituted by two rectangle-shaped radiating elements symmetrically allocated to the right and left of the feed line, as seen in Fig. 1. The feed line using a microstrip line is more suitable for the presented antenna.

The antenna's operating frequency band was defined as a 5 GHz band (i.e., 5–6 GHz), and the physical dimensions of the rectangular patch were determined using the known equations to design the rectangular patch antennas [17]. By controlling the activation and deactivation of the switching elements, the surface current distribution of the antenna will be controlled, so that the radiation direction of the antenna will be deflected. Each parasitic patch behaves as a director or reflector when the PIN diode is reverse or forward biased, respectively. The goal is to have a more directional antenna with improved gain; the principle is the same as that used for the Yagi antenna proposed in [18].

Figure 1(a) shows the first step of the proposed design and illustrates two symmetrical rectangular patches distributed to the right and left of the microstrip feed line (yellow area) and placed on the substrate top side. Using another feed line of impedance $Z_3 = 100\,\Omega$, each radiating element is connected *via* a PIN diode, to the main microstrip feed line ($Z_1 = 50\,\Omega$). The operating frequency band of the initial antenna (Antenna 1) ranges from 5.18 GHz to 5.59 GHz, and the simulated reflection coefficient value is not less than -17 dB, as plotted in Fig. 2(a). It can also be observed that Antenna 1 has a maximum simulated gain of 8 dB, as shown in Fig. 2(b). The results given in this subsection are observed when the proposed antenna is operating in state 1.

In order to make the antenna more suitable for the 5 GHz to 6 GHz frequency band and to enhance the antenna gain, a modification in the feed line form has been implemented, using a $\lambda/4$ impedance transformer, in such a way that the impedance of the second segment of the line located between the

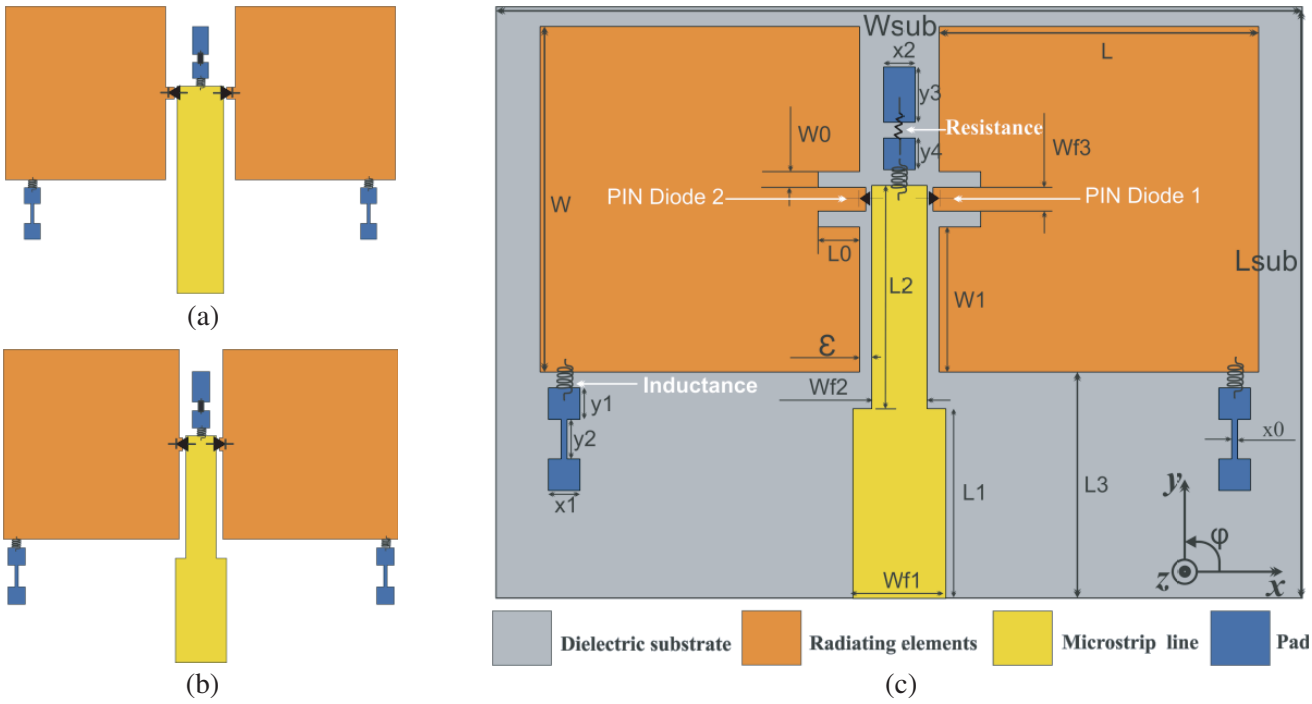

Figure 1. Evolution of antenna design: (a) Antenna 1; (b) Antenna 2; (c) Proposed antenna.

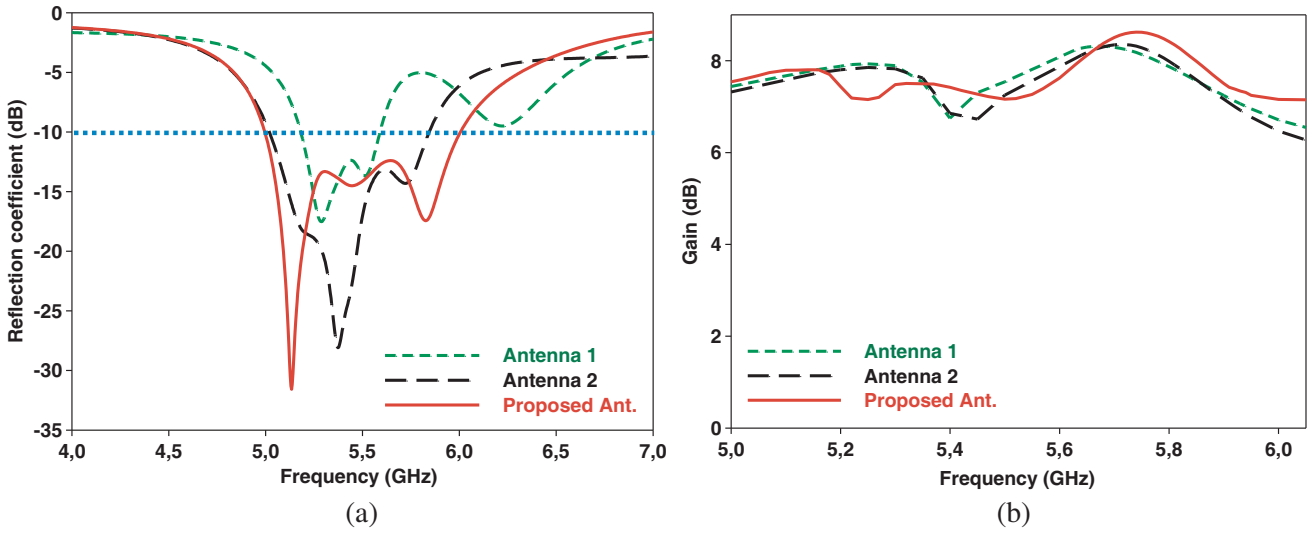

Figure 2. (a) S_{11} parameter and (b) antenna gain for the different steps.

two rectangular patches is $Z_2 = 71\,\Omega$ (Antenna 2), as shown in Fig. 1(b). The impedance of the second segment can be calculated as follows:

$$Z_2 = \sqrt{Z_1 Z_3} \tag{1}$$

As illustrated in Fig. 2(a), the operating frequency band of the second antenna (Antenna 2) ranges from 5.02 GHz to 5.84 GHz. It can also be noted that the maximum value of the simulated gain is 8.35 dB, as plotted in Fig. 2(b).

In order to increase the gain and bandwidth of the antenna, as well as the pattern reconfigurability, two I-shaped slots were inserted on both sides of the microstrip feed line in each radiating rectangular

patch, as shown in Fig. 1(c). The third segment belongs to the two rectangular patches, as illustrated in Fig. 1(c). The feed point calculation is based on the principle that the maximum power transfer would occur when the line impedance matches the patch. Each radiating slot can be considered as an equivalent parallel admittance Y, where B and G present the susceptance and conductance, respectively [17]. The slots are titled as #1 and #2.

$$Y_1{=}G_1{+}jB_1 \tag{2}$$

As slot #1 is the same as slot #2, its equivalent admittance is

$$Y_1{=}Y_2, \quad G_1 = G_2, \quad B_1 = B_2 \tag{3}$$

As $W < \lambda_0$, the conductance of a single slot can be defined as

$$G_1 = \frac{1}{90}\left(\frac{W}{\lambda_0}\right)^2 \tag{4}$$

Since the admittance of total input is real, the impedance of the resonant input is also real.

$$R_{in}\left(y=0\right) = \frac{1}{2G_1} \tag{5}$$

As shown in Fig. 1(c), the input resistance of the resonant antenna can be modified by the use of a recessed feed, set back a distance L_0 from slot #1 with a width W_0, whose characteristic impedance is given by

$$Z_3 = \frac{60}{\sqrt{\varepsilon_{re}}}\ln\left[\frac{8h}{W_{f3}} + \frac{W_{f3}}{4h}\right] \tag{6}$$

Since $Z_3 = 100\,\Omega$, the value of W_{f3} can be simple to determine. Moreover, using a modal expansion analysis, the input resistance for the trough feed is approximately expressed as follows:

$$R_{in}\left(y=L_0\right) = \frac{1}{2G_1}\cos^2\left(\frac{\pi}{L}L_0\right) = R_{in}\left(y=0\right)\cos^2\left(\frac{\pi}{L}L_0\right) \tag{7}$$

From Equation (6), the distance L_0 of each slot can be expressed as follows:

$$L_0 = \frac{L}{\pi}\cos^{-1}\left(\sqrt{\frac{R_{in}\left(L_0\right)}{R_{in}\left(0\right)}}\right) = \frac{L}{\pi}\cos^{-1}\left(\sqrt{\frac{Z_3}{R_{in}\left(0\right)}}\right) \tag{8}$$

During the design of our antenna, two matching techniques were used at the same time: the recessed microstrip-line feed and the $\lambda/4$ impedance transformer. Thus, the feed line of the proposed antenna consists of three segments with different characteristic impedances: $Z_1 = 50\,\Omega$, $Z_2 = 71\,\Omega$, and $Z_3 = 100\,\Omega$, for the first, second, and third segments, respectively. The final proposed antenna geometry is formed of two rectangle-shaped radiating cells, as shown in Fig. 1(c). Each rectangular patch element (orange area) is connected by a PIN diode with the microstrip feed line (yellow area) in the 0.3 mm wide gap between them. As Fig. 2(a) shows, the operating frequency band of the proposed antenna ranges from 5 GHz to 6 GHz. As can be observed in Fig. 2(b), the final antenna has a maximum gain of 8.62 dB at 5.8 GHz.

2.2. Parametric Study

In order to understand the effect of the dimensions of the geometry on the performance of the proposed antenna such as the gain and reflection coefficient (S_{11}), a parametric study has been carried out. We present the proposed antenna's parametric study, which is used to obtain the best performance and optimal values, by adjusting one parameter at a time while the other ones are left unchanged. All the results shown are for operating state 1.

2.2.1. Length Effect L_2

The parameter S_{11} and antenna gain were simulated as a function of various length L_2 values of the second part of the microstrip feed line, as shown in Fig. 3. It is observed that the bandwidth of the impedance of the proposed design is unchanged. As shown in Fig. 3(a), when $L_2 = 11.3\,\text{mm}$, the reflection coefficient becomes more adapted for the desired frequency range. At the same time, the antenna gain remains stable for different values of L_2, as plotted in Fig. 3(b). The length value of 11.3 mm was chosen as the optimal value L_2.

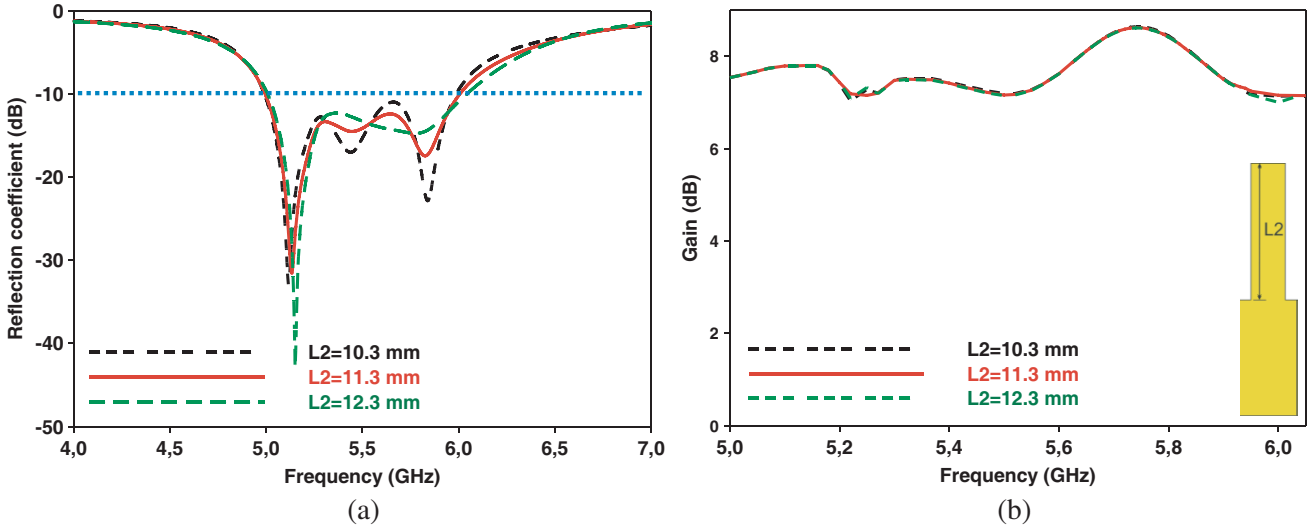

Figure 3. (a) S_{11} parameter and (b) antenna gain as a function of different values of L_2.

2.2.2. Length Effect L_0

The antenna gain and S_{11} parameter were also simulated taking into account the different values of length L_0. As can be seen in Fig. 4(a), the operating frequency band is reduced when length L_0 decreases, while the S_{11} parameter becomes increasingly unsuitable for the desired frequency band

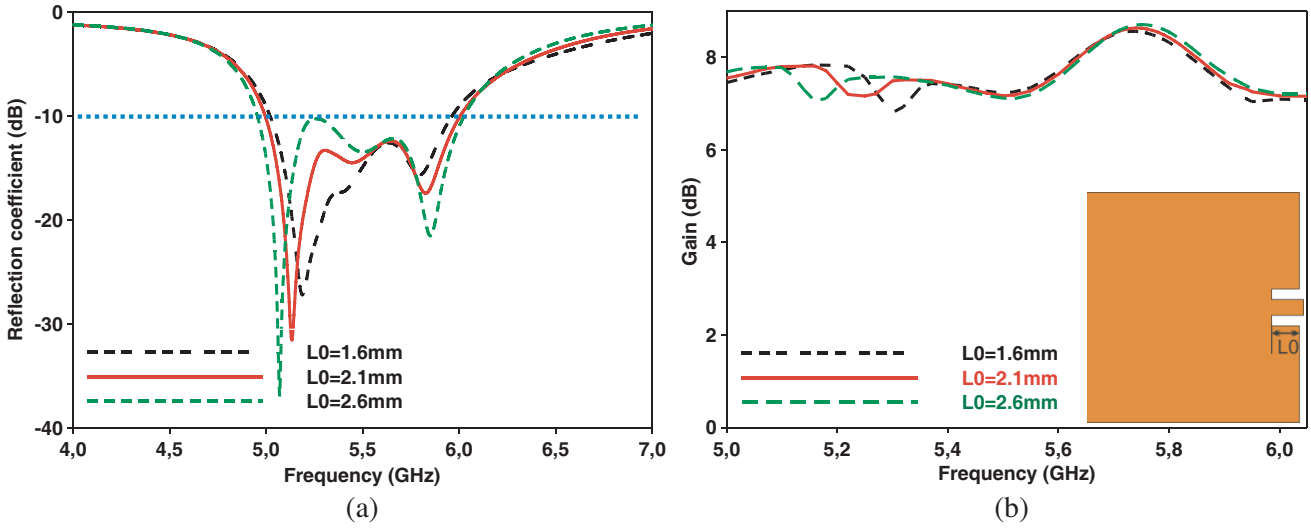

Figure 4. (a) S_{11} parameter and (b) antenna gain as a function of different values of L_0.

(5 GHz to 6 GHz) when L_0 is greater than or equal to 2.6 mm. In addition, the gain of the antenna takes its maximum (8.62 dB) at 5.8 GHz when $L_0 = 2.1$ mm, as illustrated in Fig. 4(b). It can be observed that the optimal value of L_0 has been chosen for a length of 2.1 mm.

2.2.3. Length Effect W_0

The S_{11} parameter and antenna gain were also simulated as a function of the different values of width W_0. As can be seen in Fig. 5(a), the operating frequency range remains unchanged. The S_{11} parameter becomes more adapted for the desired frequency band when the width W_0 value is 0.8 mm. As shown in Fig. 5(b), the gain of the antenna is maximum and remains unchanged at the desired frequency for all different values of W_0. The width value of 0.8 mm was selected as the optimal value W_0.

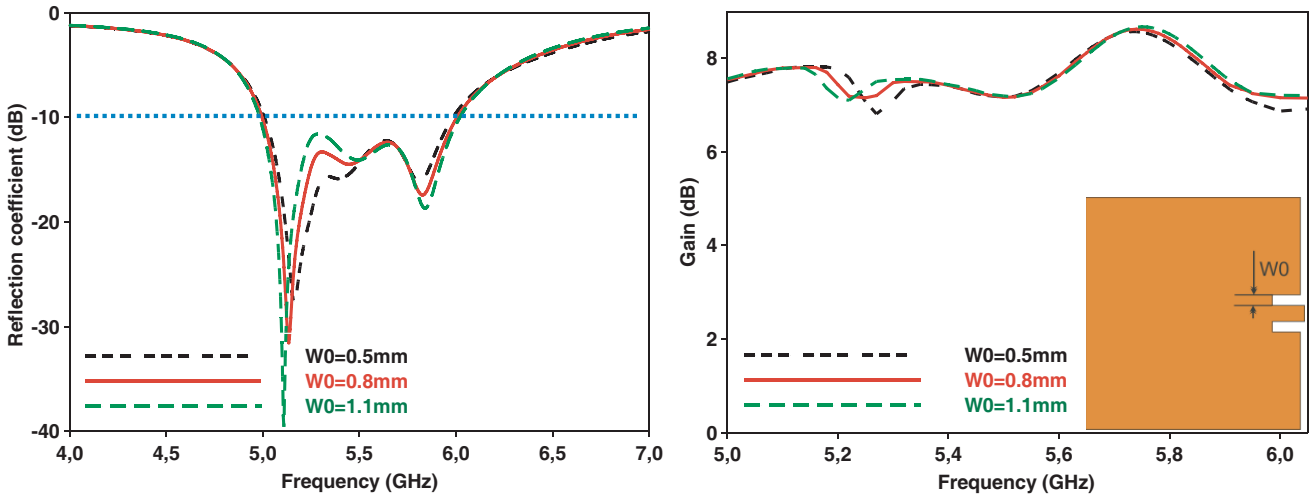

Figure 5. (a) S_{11} parameter and (b) antenna gain as a function of different values of W_0.

2.2.4. Width Effect ε

In this subsection, we show the width effect ε of the gap between the feed line and the radiating elements on the reflection coefficient and gain, while the other dimensions are kept invariant. In Fig. 6(a), the S_{11} parameter curves versus different values of ε are presented. It can be seen that the bandwidth decreases as the width ε increases, while the S_{11} parameter becomes increasingly unsuitable for the desired frequency band (5 GHz to 6 GHz) when ε is less than or equal to 0.3 mm. In parallel, it can be observed from Fig. 6(b) that the maximum value of gain at 5.8 GHz is found for $\varepsilon = 0.6$ mm. Consequently, the optimized value of ε chosen is 0.6 mm.

The proposed antenna was designed and simulated using Computer Simulation Technology (CST) Microwave Studio software. Table 1 shows the values of the optimized parameters.

Table 1. Proposed antenna dimensions.

Parameter	$\mathbf{W_{sub}}$	**W**	$\mathbf{W_0}$	$\mathbf{W_1}$	$\mathbf{W_{f1}}$	$\mathbf{W_{f2}}$	$\mathbf{W_{f3}}$
Dimension (mm)	52.5	17.5	0.8	7.35	4.7	2.8	1.2
Parameter	$\mathbf{L_{sub}}$	**L**	$\mathbf{L_0}$	$\mathbf{L_1}$	$\mathbf{L_2}$	$\mathbf{L_3}$	**E**
Dimension (mm)	40.42	16.17	2.1	9.6	11.3	11.45	0.6
Parameter	$\mathbf{x_0}$	$\mathbf{x_1}$	$\mathbf{x_2}$	$\mathbf{y_1}$	$\mathbf{y_2}$	$\mathbf{y_3}$	$\mathbf{y_4}$
Dimension (mm)	0.3	1.6	1.6	1.6	2	2.8	1.6

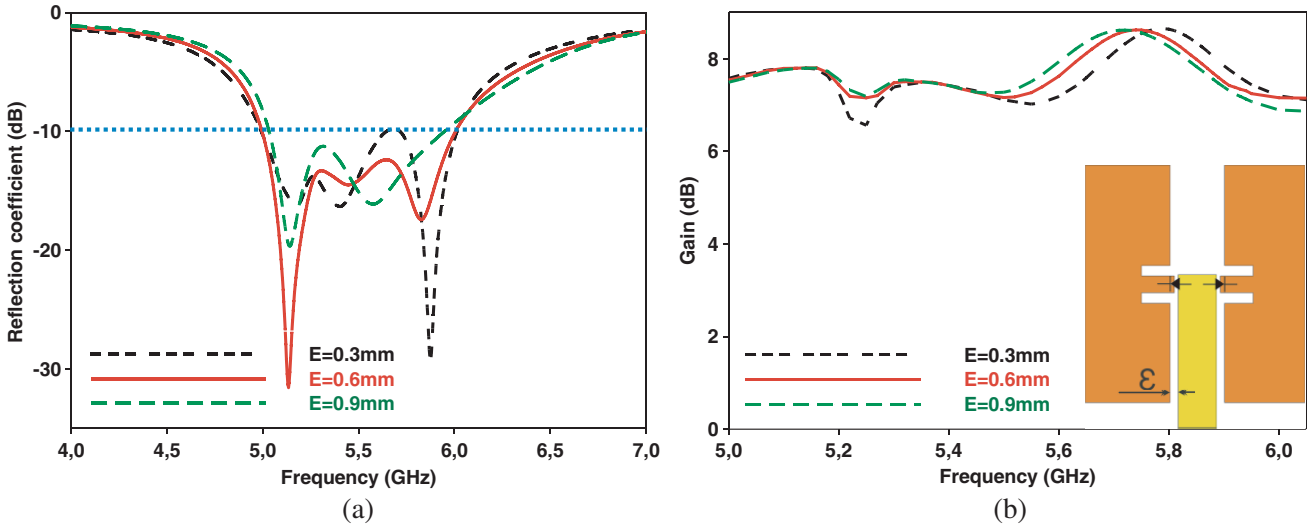

Figure 6. (a) S_{11} parameter and (b) antenna gain as a function of different values of ε.

2.3. Equivalent Circuit Model

Based on the datasheet, the parameters of the PIN diode MPP4203 are $L_D = 0.02\,\text{nH}$, $R_{DS} = 3\,\Omega$, $C_T = 0.08\,\text{pF}$, and $R_{DP} = 25\,\text{K}\Omega$. Figs. 7(a)–(b) show the RF equivalent circuits of the PIN diode for both states ON and OFF, respectively [19]. To control the PIN diodes states, DC bias circuits were used as drawn in Fig. 7(c). Changing the PIN diodes ON-OFF states, the designed antenna achieves pattern reconfigurability. Since DC current does not affect the controlled element, the influence of capacitors

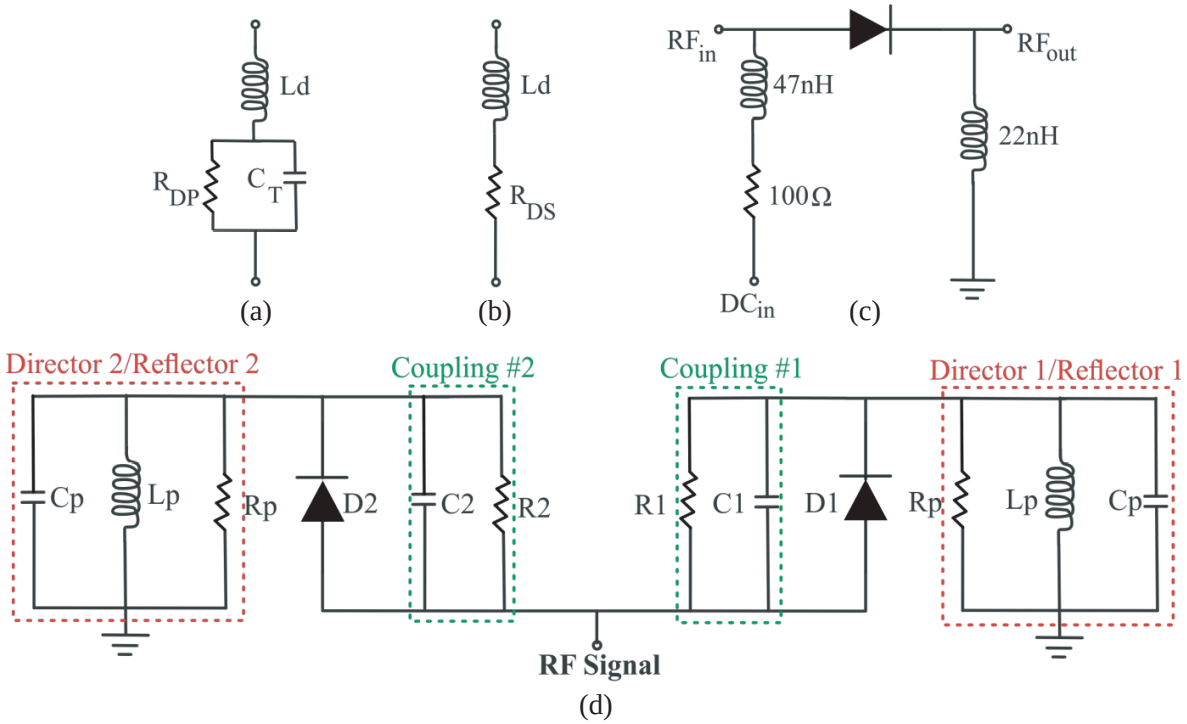

Figure 7. Equivalent circuit model: (a) PIN diode reverse bias (OFF); (b) PIN diode forward bias (ON); (c) DC bias circuit; (d) Proposed antenna.

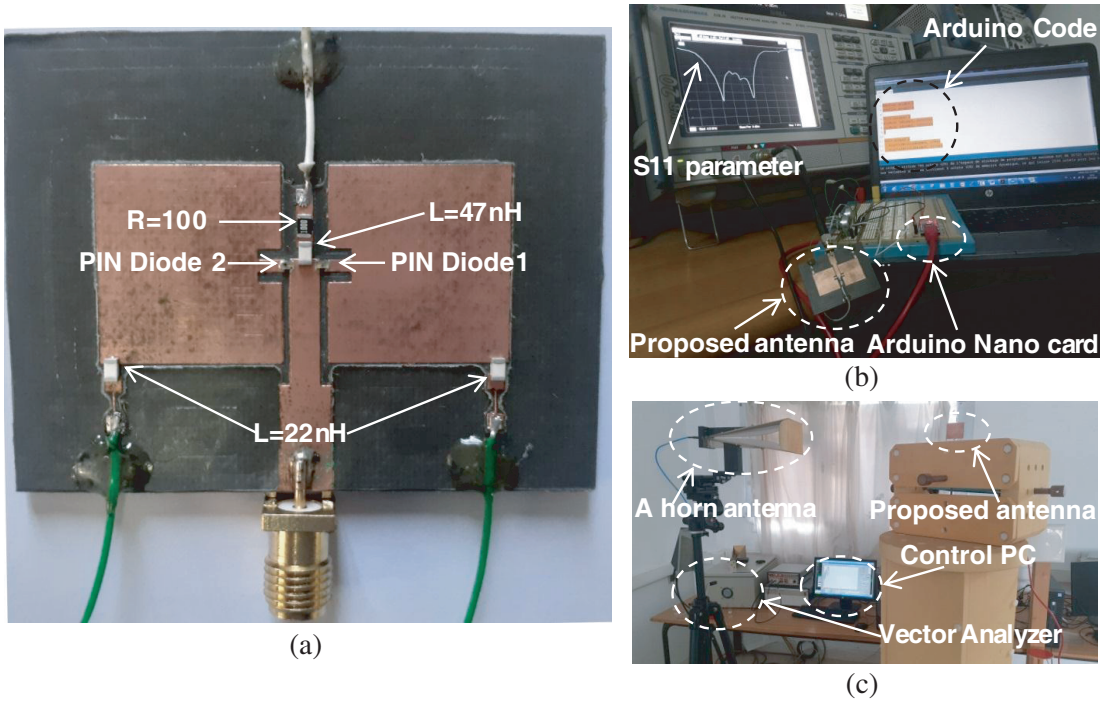

Figure 8. (a) Fabricated prototype photograph. (b) Measurement of S_{11} parameter. (c) Far-field proposed antenna measurement setup.

remains negligible in DC circuits. In order to not alter the current circulating into the bias circuit on the patch element, two inductances 47-nH and 22-nH are required. By monitoring the DC voltages, the states of the PIN diodes are commutated. When the DC in value is 2 V, the PIN diode turns on, while if the DC in value is 0 V, the diode is deactivated. Accordingly, each radiating element will act as a director or as a reflector. The DC bias circuit was powered by an Arduino Nano card as illustrated in Fig. 8(b).

As shown in Fig. 7(d), a rectangular microstrip patch can be viewed as a parallel arrangement of capacitance (C_P), inductance (L_P), and resistance (R_P). The expressions defining the localized elements of $R_P L_P$ and C_P [20] are given as:

$$C_P = \frac{\varepsilon_0 \varepsilon_{re} LW}{2h} \cos^{-2}\left(\frac{\pi Y_f}{L}\right) \tag{9}$$

$$L_P = \frac{1}{\omega_P^2 C_P} \tag{10}$$

$$R_P = \frac{Q_r}{\omega C_P} \tag{11}$$

where L and W represent the length and width of the patch, respectively. $Y_f = y$ corresponds to the feed point coordinate, and h represents the substrate material thickness.

$$Q_r = \frac{c\sqrt{\varepsilon_{re}}}{4fh} \tag{12}$$

The proposed reconfigurable antenna equivalent circuit is shown in Fig. 7(d). Taking into account the inter-element couplings, the gaps between the microstrip feeder and each of the two rectangular patches shown in Fig. 1(c) can be viewed as a parallel combination of a capacitor (C_1) and a resistor (R_1) (coupling #1) and a parallel combination of a capacitor (C_2) and a resistor (R_2) (coupling #2), respectively. The Advanced Design System (ADS) was used to simulate the equivalent circuit of the proposed antenna. The final optimized values of the lumped parameters are given in Table 2.

Table 2. Optimized values of the lumped parameters.

Parameter	C_P	R_P	L_P	C_1	R_1	C_2	R_2
Value	2.72 pF	90 Ω	0.268 nH	0.33 pF	900 Ω	0.33 pF	900 Ω

3. RESULTS AND DISCUSSION

A printed circuit board (PCB) milling machine (The LPKF Protomat E33) is used to fabricate the antenna shown in Fig. 1(c). Two bias lines are used to control each PIN diode; one is used as a DC supply and the other as a ground, as shown in Fig. 8(a). As can be seen in Fig. 9, the activation of one of the PIN diodes modifies the surface current distribution of the antenna, which deflects the radiation direction of the antenna. As a result, the specific bias requirements for the possible operating states are shown in Table 3. When the PIN diode is reverse biased, the radiating element acts as a director. If not, it behaves as a reflector, and thus the antenna system forms a 180° phase shift directional radiation pattern in the azimuth plane. It can be seen that the proposed antenna operates in three different states named S1, S2, and S3.

Table 3. Proposed antenna operating conditions.

Operating states	PIN Diodes states		Bandwidth (GHz)	Simulated Gain (dB)	Beam direction		
	D1	D2			E-plane	H-plane	Azimuth-plane
State 1	OFF	ON	5.0 to 6.0	8.62	$\theta = 12°$	$\theta = 30°$	$\Phi = 0°$
State 2	ON	OFF	5.0 to 6.0	8.62	$\theta = 12°$	$\theta = -30°$	$\Phi = 180°$
State 3	ON	ON	5.74 to 5.86	6.71	$\theta = -3°$	$\theta = -38°$ & $\theta = 38°$	$\Phi = 0°$ & $\Phi = 180°$

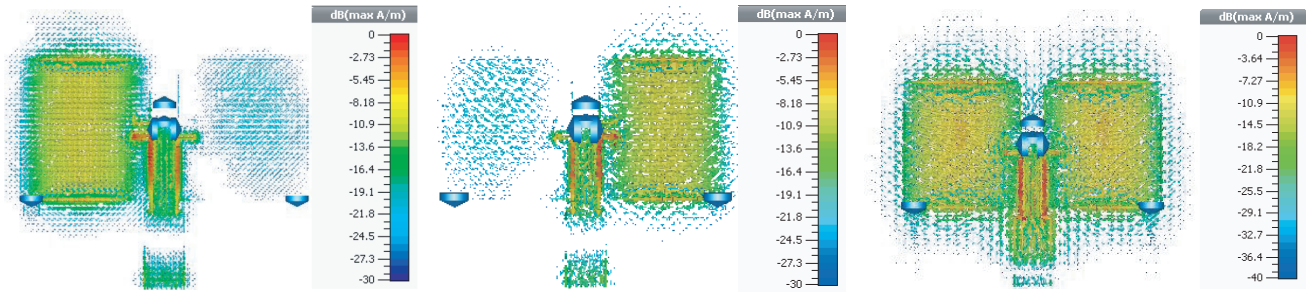

(a) (b) (c)

Figure 9. Surface current distribution at 5.8 GHz: (a) State 1; (b) State 2; (c) State 3.

As shown in Fig. 8(b), the reconfigurable antenna's reflection coefficient was measured using the "Rohde and Schwarz ZVB20" Vector Network Analyzer to check the results obtained by simulation. The comparison of the simulated, theoretical, and measured results of S_{11} parameter is presented in Fig. 10(a). For states 1 and 2, the simulated fractional bandwidth is 18.18% from 5.0 to 6.0 GHz; the theoretical one is 18.84% from 5 to 6.04 GHz; and the measured result is 19.42% from 5.02 to 6.10 GHz. On the other hand, as mentioned in Fig. 10(b), for state 3, the antenna bandwidth is 2.1% from 5.74 to 5.86 GHz (simulated), 3.1% from 5.68 to 5.86 GHz (theoretical), and 3.2% from 5.72 to 5.91 GHz (measured). The results of the simulations are slightly different from the experimental results, which can be attributed to the tolerances of the manufacturing process. In fact, the three different results can

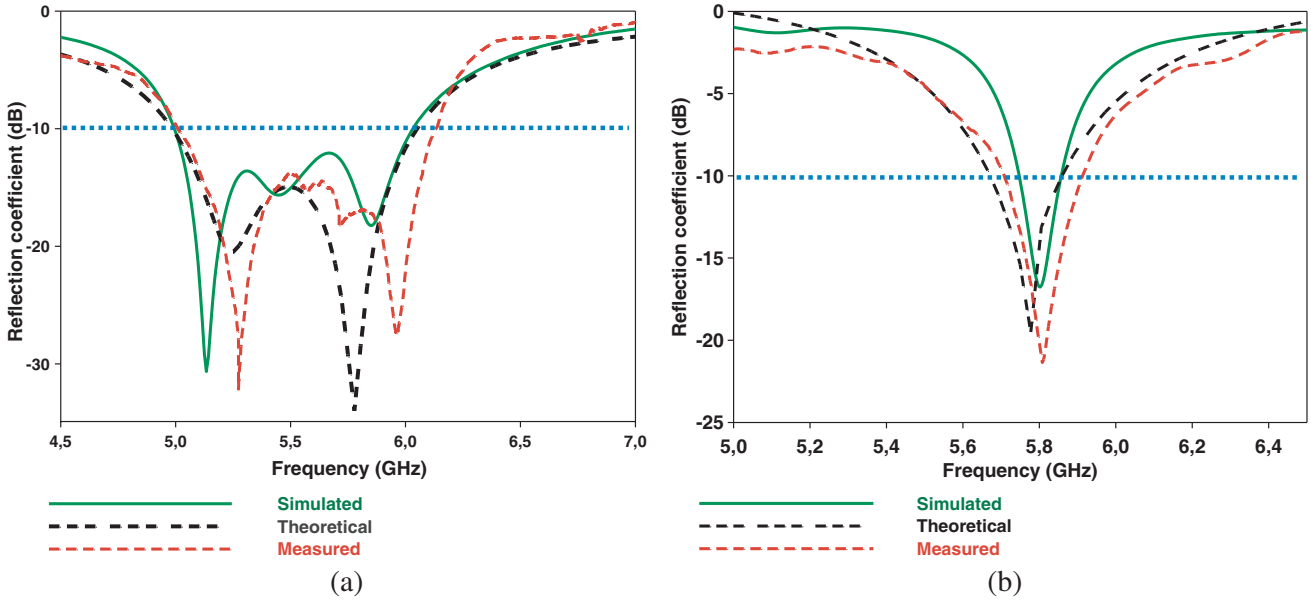

Figure 10. S_{11} parameter: (a) State 1 and state 2; (b) State 3.

be seen to match up well. This enhanced bandwidth can be explained by the use of smaller capacity electronic switches and the use of two I-shaped slots in each rectangular patch radiating as indicated in Fig. 1(c).

For both states 1 and 2, as the frequency increases in the operating band (5–6 GHz), the radiation efficiency increases from 80% to 86%, while for state 3, the radiation efficiency increases up to 85% in the operating frequency range, as shown in Fig. 11. For the first two operating states (S1 and S2), the antenna owns a maximum simulated gain of 8.62 dB and a maximum measured gain of 8.45 dB, whereas for state 3, the maximum simulated gain is 6.71 dB, and the maximum measured gain is 6.12 dB. This high efficient and improved antenna gain for the first two operating states is due to the use of one radiating cell as director and another radiating cell as reflector for each state, and to the use of a Rogers RT5880 dielectric with a low loss tangent of 0.0009.

As mentioned in Fig. 8(c), the measurements of the far field radiation patterns are made by an antenna measurement system from Geozondas Ltd. The measured and simulated E-plane radiation

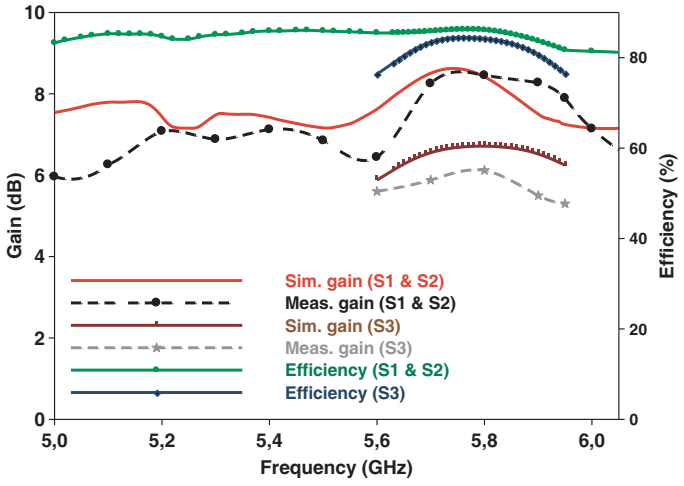

Figure 11. Simulated antenna gain and radiation efficiency.

patterns are shown in Figs. 12(a)–(c). The principal beam of the antenna can be directed at about 12° for both state 1 and state 2, while for state 3, the antenna beam can be steered to about −3° in the E-plane. The radiation patterns in the simulated and experimental H-planes are shown in Figs. 12(d)–(f). It is possible to direct the main beam of the antenna to approach 30° (right end-fire) and −30° (left end-fire) for states 1 and 2, respectively, whereas for state 3, the antenna beam can be directed to about 38° (right endfire) and −38° (left endfire) at the same time. From the radiation patterns in the E-plane and H-plane at the frequency of 5.8 GHz, it can be seen that the proposed antenna radiates in three different directions. The designed antenna has a directional perfect pattern in the E-plane and a bidirectional and directional pattern in the H-plane at 5.8 GHz. However, the measurements agree well with the predictions of the simulation, which validate the operation of the antenna.

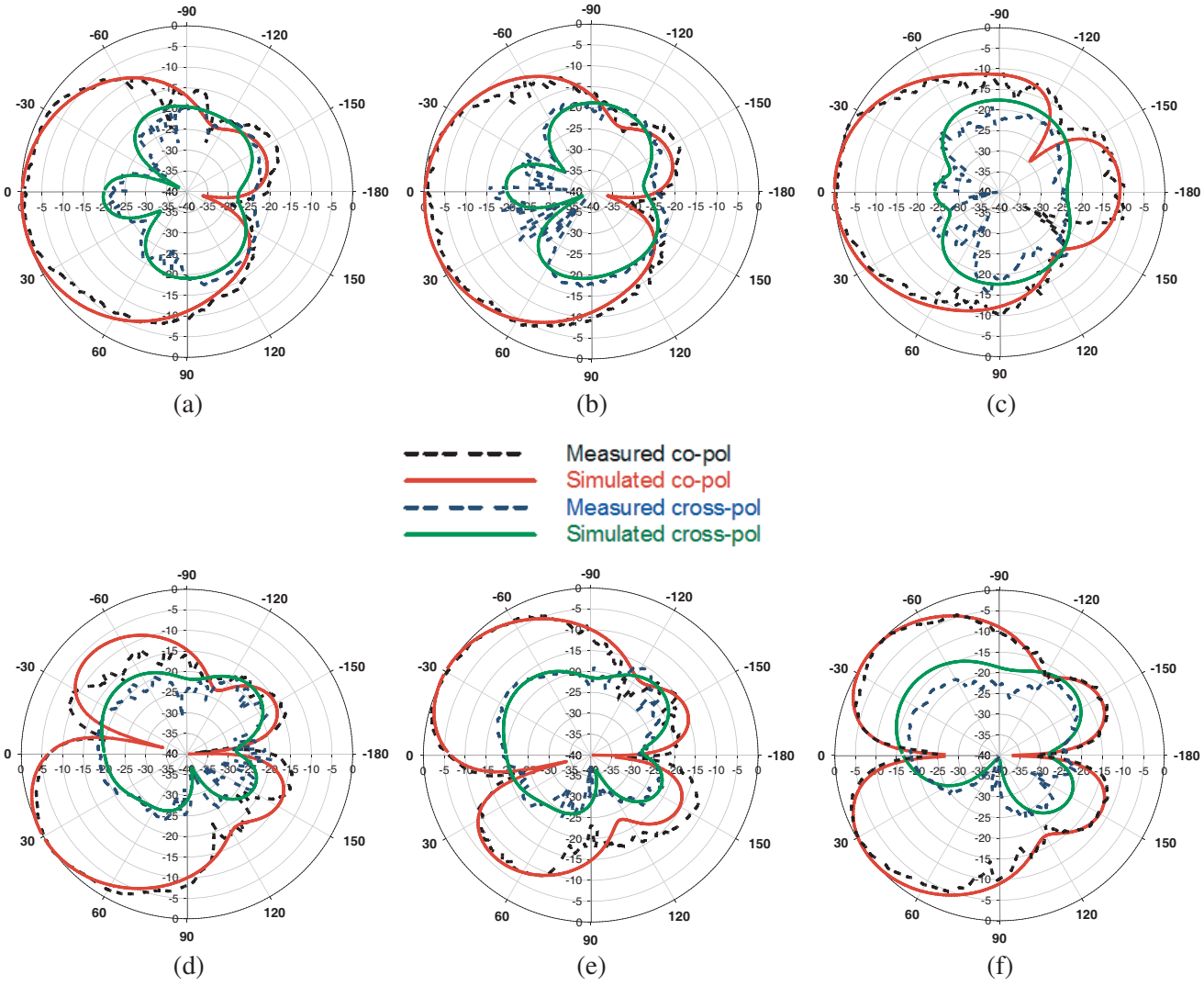

Figure 12. Proposed antenna radiation patterns (E-plane and H-plane at 5,8 GHz): (a) State 1 in E-plane; (b) State 2 in E-plane; (c) State 3 in E-plane; (d) State 1 in H-plane; (e) State 2 in H-plane; (f) State 3 in H-plane.

In order to validate the proposed design, a comparison of our reconfigurable antenna with other related designs reported previously is shown in Table 4. In addition to pattern reconfigurability and improved impedance bandwidth, the proposed antenna has other advantages including improved gain, high efficiency, and reduced size.

Table 4. Proposed antenna compared to several recent published works.

Year/Ref.	No. of switches	No. of layers	Size (λ^3)	Frequency (GHz)	BW (%)	Peak gains (dBi)	Efficiency (%)
2019/[21]	8	1	$1.48 \times 1.48 \times 0.008$	2.34	10.25	5.9	NG
2020/[22]	6	1	$0.91 \times 0.85 \times 0.02$	3.65	4.1	5.7/6.9	89
2020/[23]	12	4	$1.39 \times 1.39 \times 0.06$	2.45	12.24	7.0/8.9	NG
2021/[24]	2	1	$0.22 \times 0.27 \times 0.001$	1.80	41	2.2	80
2021/[25]	14	3	$0.59 \times 0.53 \times 0.08$	2.4/5.8	2.07/2.6	6.2/6.6	NG
Proposed	**2**	**1**	$0.67 \times 0.53 \times 0.03$	**5.80**	**18.18**	**6.71/8.62**	**86**

λ_0: wavelength of the free space.
NG: not given.

4. CONCLUSION

In this work, an adjustable Broadband Radiation Pattern Microstrip Antenna is studied, simulated, and measured. The presented antenna is capable of operating in three different basic states, achieving a reconfigurable radiation characteristic based on the switching bias of the PIN diode. By changing the surface current distribution of the antenna, the radiation direction of the antenna will be deflected in three different directions in the elevation plane. As a result, a wide angle beams switching property ranging from ($\pm 30°$) to ($\pm 38°$) in an elevation plane can be obtained through a simple and inexpensive approach using no additional conventional circuits. This means that the antenna has the possibility to cover the complete azimuth plane. The designed reconfigurable antenna presents good radiation characteristics along with a high gain (up to 8.62 dB), wide bandwidth to cover the complete 5 GHz band spectrum (i.e., 5–6 GHz), and a very good efficiency of 86%. Thus, the designed reconfigurable antenna perfectly meets the objective of this work.

REFERENCES

1. George, R. and T. A. J. Mary, "Review on directional antenna for wireless sensor network applications," *IET Communications*, Vol. 14, 715–722, 2020.
2. Ojaroudi Parchin, N., H. Jahanbakhsh Basherlou, Y. Al-Yasir, R. Abd-Alhameed, et al., "Recent developments of reconfigurable antennas for current and future wireless communication systems," *Electronics*, Vol. 8, 128, 2019.
3. Mohamadzade, B., R. B. V. B. Simorangkir, S. Maric, A. Lalbakhsh, et al., "Recent developments and state of the art in flexible and conformal reconfigurable antennas," *Electronics*, Vol. 9, 1375, 2020.
4. Kamran Shereen, M., M. I. Khattak, and G. Witjaksono, "A brief review of frequency, radiation pattern, polarization, and compound reconfigurable antennas for 5G applications," *J. Comput. Electron.*, Vol. 18, 1065–1102, 2019.
5. Singh, A., R. Dubey, R. Jatav, and M. K. Meshram, "Electronically reconfigurable microstrip antenna with steerable beams," *AEU — International Journal of Electronics and Communications*, Vol. 149, 154179, 2022.
6. Haider, N., D. Caratelli, and A. G. Yarovoy, "Recent developments in reconfigurable and multiband antenna technology," *International Journal of Antennas and Propagation*, Vol. 2013, 1–14, 2013.
7. Ojaroudi Parchin, N., H. Jahanbakhsh Basherlou, Y. I. A. Al-Yasir, A. M. Abdulkhaleq,, et al., "Reconfigurable antennas: Switching techniques — A survey," *Electronics*, Vol. 9, 336, 2020.
8. Al Abbas, E., N. Nguyen-Trong, A. T. Mobashsher, and A. M. Abbosh, "Polarization-reconfigurable antenna array for millimeter-wave 5G," *IEEE Access*, Vol. 7, 131214–131220, 2019.

9. Zhang, Z., S. Cao, and J. Wang, "Azimuth-pattern reconfigurable planar antenna design using characteristic mode analysis," *IEEE Access*, Vol. 9, 60043–60051, 2021.
10. Jin, G., M. Li, Y. Xu, J. Yang, et al., "Differentially fed six-beam switchable reconfigurable antenna," *IET Microwaves, Antennas & Propagation*, Vol. 14, 573–577, 2020.
11. Zahra, H., M. Hussain, S. I. Naqvi, S. M. Abbas, et al., "A simple monopole antenna with a switchable beam for 5G millimeter-wave communication systems," *Electronics*, Vol. 10, 2870, 2021.
12. Deng, Z., X. Guo, H. Wei, J. Gan, et al., "Design, analysis, and verification of Ka-band pattern reconfigurable patch antenna using RF MEMS switches," *Micromachines*, Vol. 7, 144, 2016.
13. Hu, J., X. Yang, L. Ge, Z. Guo, et al., "A reconfigurable 1×4 circularly polarized patch array antenna with frequency, radiation pattern, and polarization agility," *IEEE Trans. Antennas Propagat.*, Vol. 69, 5124–5129, 2021.
14. Shang, Y., Q. Zeng, W. Cui, X. Wang, et al., "Design of pattern reconfigurable patch antenna array based on reflective phase-shifter," *International Journal of Antennas and Propagation*, Vol. 2022, 1–10, 2022.
15. Karam, M. Y. and R. M. Jafar, "Array pattern reconfiguration using pixel method," *The Applied Computational Electromagnetics Society Journal*, Vol. 35, 273–278, 2020.
16. Faouzi, R., A. T. Naima, B. Abdelmounaim, A. Noura, et al., "Pattern reconfigurable antenna for VANET, Wi-Fi, and WiMAX wireless communication systems," *International Journal of Antennas and Propagation*, Vol. 2021, 1–12, 2021.
17. Balanis, C. A., *Antenna Theory: Analysis and Design*, 3rd Edition, John Wiley, Hoboken, 2005.
18. Mohammed, J. R., "Design of printed Yagi antenna with additional driven element for WLAN applications," *Progress In Electromagnetics Research C*, Vol. 37, 67–81, 2013.
19. Datasheet of Microsemi MPP4203 PIN Diodes: http://www.microsemi.com (accessed on March 19, 2022).
20. Garg, R., P. Bhartia, I. J. Bahl, and A. Ittipiboon, *Microstrip Antenna Design Handbook*, Artech House, Norwood, Mass., USA, 2000.
21. Lee, S. J., W. S. Yoon, and S.-M. Han, "Planar beam steerable parasitic array antenna system design based on the Yagi-Uda design method," *International Journal of Antennas and Propagation*, Vol. 2019, 1–9, 2019.
22. Gaya, S., R. Hussain, M. S. Sharawi, and H. Attia, "Pattern reconfigurable Yagi-Uda antenna with seven switchable beams for WiMAX application," *Microw. Opt. Technol. Lett.*, Vol. 62, 1329–1334, 2020.
23. Kang, L., H. Li, J. Zhou, and S. Zheng, "An OAM-mode reconfigurable array antenna with polarization agility," *IEEE Access*, Vol. 8, 40445–40452, 2020.
24. Ghaffar, A., X. J. Li, W. A. Awan, A. H. Naqvi, et al., "A flexible and pattern reconfigurable antenna with small dimensions and simple layout for wireless communication systems operating over 1.65–2.51 GHz," *Electronics*, Vol. 10, 601, 2021.
25. Ismail, M. F., M. K. A. Rahim, M. R. Hamid, H. A. Majid, and B. S. Nugroho, "Dual-band pattern reconfigurable antenna using electromagnetic band-gap structure," *AEU — International Journal of Electronics and Communications*, Vol. 130, 153571, 2021.